

Exploiting Silicon-on-Insulator Microring Resonator Bistability Behavior for All Optical Set-Reset Flip-Flop

P. Nadimi, D. D. Caviglia, and E. Di Zitti

Abstract—We propose an all optical flip-flop circuit composed of two Silicon-on-insulator microring resonators coupled to straight waveguides by exploiting the optical bistability behavior due to the nonlinear Kerr effect. We used the transfer matrix analysis to investigate continuous wave propagation through microrings, as well we considered the nonlinear switching characteristics of an optical device using a double-coupler silicon ring resonator in presence of the Kerr nonlinearity, thus obtaining the bistability behavior of the output port, the drop port and also inside the silicon microring resonator. It is shown that the bistability behavior depends on the control of the input wavelength.

Keywords—All optical flip-flops, Kerr effect, microring resonator, optical bistability.

I. INTRODUCTION

OPTICAL flip-flops made with optical resonators are the fundamental building blocks of optical sequential logic circuits [1] that could be used for memory and buffering applications [2].

Flip-flops are basic electronic devices to store information, used as elementary processing units, and represent an example of competitive bistable systems [3].

In optical domain, optical resonator structures can store light for short periods of time, due to the extremely short photon lifetime [3]. Many researches on all-optical memories with logic gates with semiconductor microresonators [4], bistable laser diodes [5], nonlinear polarization switches [6], coupled polarization switches [7], and set-reset flip-flops by fiber loop resonators [8], nonlinear effects of coupled microring resonators and waveguide [3] have been shown. Moreover, an all-optical flip-flop memory based on the optical bistability of a microring resonator was reported [9]. Optical bistability in a resonator allows the construction of all optical flip-flops and other devices exhibiting dynamic optical memory [10], [11].

This effect in microrings has been theoretically and experimentally studied [1], [12], and a unified analytical theory for optical bistability inside microring resonator has been developed [11].

P. Nadimi, Diten, University of Genoa, Genoa, Italy (pantea.nadimi@unige.it).

D.D. Caviglia, Diten, University of Genoa, Genoa, Italy (daniele.caviglia@unige.it)

E. Di Zitti, Diten, University of Genoa, Genoa, Italy (dizitti@unige.it).

All-optical high-speed flip-flop circuits can be realized by exploiting the Kerr nonlinear effect since it allows much faster switching speeds than those achieved by using free-carrier or thermal nonlinearities [13], [14].

In this framework, we propose an implementation of an all optical set-reset flip-flop based on the optical bistability behavior of silicon microring resonators due to the nonlinear Kerr effect.

II. PROPOSED DESIGN

We propose to use two continuous wave (CW) signals, set and reset, and two silicon base microrings. Figure 1 depicts the structure, where $L_1 = 10 \mu\text{m}$ and $L_2 = 20 \mu\text{m}$ are the lengths of the straight waveguides before and after the coupling points of microrings MR1 and MR2, where MR1 has a bistable behavior, while MR2 does not operate in the bistability region.

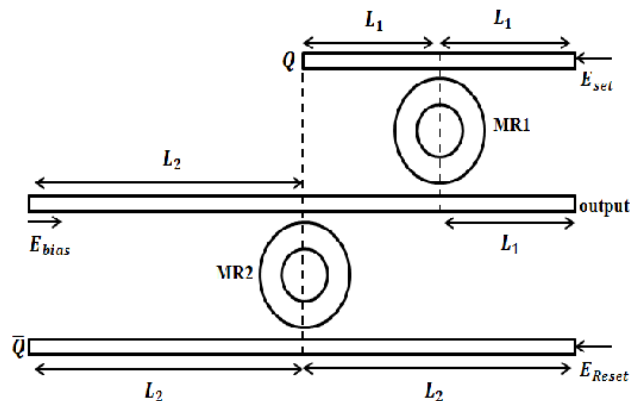


Fig. 1 Schematic of the proposed optical flip flop

Following [15], by using two silicon-on-insulator (SOI) microring resonators (MR1 and MR2) with the same radius, $5 \mu\text{m}$, and coupled to a set of waveguides, an all optical set-reset flip-flop can be realized. The optical parameters of MR1 are therefore chosen to get such a bistable device.

In the proposed implementation, the Set beam in input to the upper straight waveguide is a CW signal at 1550 nm with incident intensity $I_{in} = 2.38 \text{ GW/cm}^2$, which is slightly detuned to the resonance wavelength of MR1, thus causing the bistability behavior of MR1. The Reset beam in input to the lower straight waveguide is a CW signal at 1518 nm with

incident intensity $I_{in} = 2.05 \text{ GW/cm}^2$, which is tuned to the resonance wavelength of MR2; in this way, the ring bistability behavior will completely disappear as MR2 has not hysteresis. The bias signal in input to the mid straight waveguide is a CW signal at 1561.94 nm; it is worth noting that it is initially red tuned to the resonance wavelength of both MR1 and MR2, as well the bias beam intensity should be kept at a level low enough not to excite nonlinear effects.

The optical flip-flop operation will be expressed by the transmission of the CW bias to the Q or \bar{Q} ports.

III. OPTICAL BISTABILITY INDUCED BY KERR

We will follow the theoretical analysis [15] of the consequence of linear loss and nonlinear Kerr effect simultaneously on the nonlinear switching in the double coupler nonlinear SOI microring resonator, combined with transfer matrix analysis (TMA) to assess the behavior of the proposed structure. While TMA efficiently gives the system behavior based on the coupling coefficients between the waveguides and the microrings, investigating the nonlinear switching in the double coupler nonlinear microring resonators let us to assess the bistability of microrings. Vanishkorn et al. [15] have investigated the nonlinear switching characteristics of an optical device using a double-coupler silicon ring resonator in the presence of the linear losses, the Kerr nonlinearity, two-photon absorption (TPA), free-carrier-induced absorption and dispersion, and thermo-optic effect. Using the same notation for considering a CW signal at a wavelength λ propagating inside a straight SOI waveguide coupled laterally to a silicon microring of radius R as in [11], [15], the evolution of the electric field E_z associated with this optical wave can be described according to a nonlinear differential equation:

$$\frac{1}{A} \frac{dA}{dz} = -\frac{\alpha}{2} - \left(\frac{\beta}{2} - i\gamma\right) |A|^2 - \left(\frac{\xi_r}{2} + i\xi_i\right) |A|^4 \quad (1)$$

$A(z)$ is the complex amplitude, $|A|^2$ represents its intensity, related to the electric field as $E_z = \tilde{\omega} A(z) e^{i\beta_0 z}$ with $\tilde{\omega} = \left(\frac{\mu_0}{\varepsilon_0}\right)^{1/4} (2n_0)^{3/2}$, where μ_0 and ε_0 are the intrinsic permeability and permittivity of vacuum, respectively; $\beta_0 = n_0 k$ is the propagation constant with $k = \frac{\omega}{c}$ where ω is the angular frequency of CW signal, n_0 is the linear refractive index, and c is the speed of light in vacuum. The parameters entering "(1)," are as follows: α , β and $\gamma = kn_2$ govern linear losses, two-photon absorption, and the Kerr effect, n_2 being the nonlinear Kerr parameter.

The parameters ξ_r and ξ_i account for the free-carrier effects and are defined as follow:

$$\xi_r = \frac{\sigma\tau\beta}{2\hbar\omega}, \quad \xi_i = \left(\frac{\mu}{2}\right) \xi_r, \quad \mu = \frac{2k\sigma n}{\sigma_r} \quad (2)$$

where $\sigma = \sigma_r \left(\frac{\omega_r}{\omega}\right)^2$ with $\sigma_r = 1.45 \times 10^{-21} \text{ m}^2$, $\omega_r =$

$\frac{2\pi c}{1.55 \times 10^{-6}} \text{ Hz}$, and $\sigma_n = 5.3 \times 10^{-27} \text{ m}^3$ and τ is the effective free-carrier life-time [11], [16]. A schematic diagram of a double coupler nonlinear ring resonator and details of the notation used is depicted in Fig. 2.

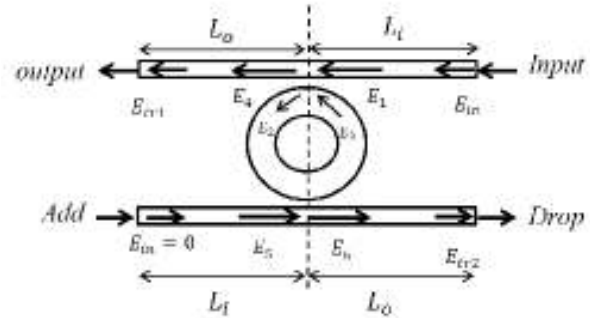


Fig. 2 Schematic of the double coupler ring resonator and details of the notation employed

Nonlinear Kerr effect, two-photon absorption and thermo-optic effects, which cause the change of the refractive index, can induce the bistability behavior in the microring resonators [9], [15]. In this paper, the only effect considered is nonlinear Kerr effect, as the impact of TPA on the attenuation of optical wave is relatively small compared with other loss sources [11].

The evolution of the electric field of "(1)," with $\beta = 0$ in the form of $A(z) = \sqrt{I(z)} e^{i\phi(z)}$ along both the straight ring waveguides in Fig. 2, is given by [15], show in "(3),":

$$I(z) = \frac{I_0 e^{-\alpha z}}{\sqrt{1 + I_0^2 \left(\frac{\xi_r}{\alpha}\right) [1 - e^{-2\alpha z}]}} \quad (3a)$$

$$\phi(z) = \phi_0 + \gamma I_0 L_{eff}(z) - \frac{\xi_i}{\xi_r} \left(\ln \frac{I_0}{I(z)} - \alpha z\right) \quad (3b)$$

$$L_{eff}(z) = \frac{\tan^{-1} \left| I_0 \sqrt{\frac{\xi_r}{\alpha}} \right| - \tan^{-1} \left| I(z) \sqrt{\frac{\xi_r}{\alpha}} \right|}{I_0 \sqrt{\xi_r \alpha}} \quad (3c)$$

where I_0 and ϕ_0 are the values of intensity and phase at $z = 0$ and L_{eff} is the generalized effective length. Coupling between the input/output signals and the circulating field in the microring at point $z = 0$ is described by :

$$E_4 = rE_1 + i\chi E_3 \quad (4a)$$

$$E_2 = rE_3 + i\chi E_1 \quad (4b)$$

$$E_3 = rE(2\pi R) \quad (4c)$$

$$E_6 = i\chi E(\pi R) \quad (4d)$$

$$E_5 = 0 \quad (4e)$$

where χ and r are the field coupling and transmission

coefficients between the straight ring waveguides such that $\chi^2 + r^2 = 1$, for lossless coupling.

By eliminating E_1 from “(4a),” and “(4b),” and noting that $E_3 = rE(2\pi R)$, the intensity I_4 has been expressed by [15], $I_4 = |E_4|^2/\tilde{\omega}^2$ in terms of $I_0 = |E_2|^2/\tilde{\omega}^2$ as,

$$I_4 = \left| \frac{r^2 [I_0 + I(2\pi R)] - 2\sqrt{I_0 I(2\pi R)} \cos \Delta\phi}{(1 - r^2)} \right| \quad (5)$$

where $\Delta\phi = 2\pi R\beta_0 + \phi(2\pi R) - \phi_0$ is the phase shift acquired during one round trip within the ring; a similar relation for the intensity I_6 can be obtained from “(4d),” and “(4e),” by [15]:

$$I_6 = \chi^2 I(\pi R) = (1 - r^2) I(\pi R) \quad (6)$$

According to the energy conservation law:

$$I_1 = I_0 + I_4 - (r^2 I(2\pi R)) \quad (7)$$

As L_i and L_o are the lengths of the straight waveguides before and after the coupling points (see Fig. 2), the intensities at the input and output ends of the straight waveguides can be related to I_1 and I_4 by:

$$I_{in}(I_0) = \frac{I_1(I_0)e^{\alpha L_i}}{\sqrt{1 + I_1^2(I_0)\left(\frac{\xi_r}{\alpha}\right)[1 - e^{2\alpha L_i}]}} \quad (8a)$$

$$I_{tr1}(I_0) = \frac{I_4(I_0)e^{-\alpha L_o}}{\sqrt{1 + I_4^2(I_0)\left(\frac{\xi_r}{\alpha}\right)[1 - e^{-2\alpha L_o}]}} \quad (8b)$$

$$I_{tr2}(I_0) = \frac{I_6(I_0)e^{-\alpha L_o}}{\sqrt{1 + I_6^2(I_0)\left(\frac{\xi_r}{\alpha}\right)[1 - e^{-2\alpha L_o}]}} \quad (8c)$$

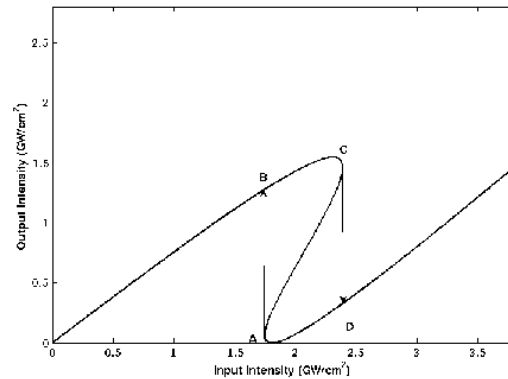
Equations “(8),” give the evolution of the input-output relation in a parametric form, where the parameter I_0 lies in the interval $[0, \infty]$. By noting that $E_2 = E(0)$, we can also earn the intensity inside the microring.

IV. RESULTS

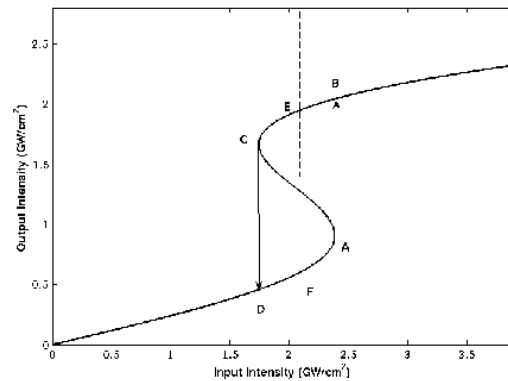
A more direct evidence of the ring bistability is the observation of a hysteresis loop in the transfer function, output power versus input power, of the ring resonator [12], [17], [18].

To illustrate such a bistable behavior, we focus on a silicon ring resonator with $5\mu\text{m}$ radius, and set $L_i = L_o = 10\mu\text{m}$ (see Fig. 2) and $n_0 = 3.48$, $\alpha = 1 \text{ dB/cm}$, $\beta = 0.5 \text{ cm/GW}$, $n_2 = 6 \times 10^{-5} \text{ cm}^2/\text{GW}$, $\tau = 1 \text{ ns}$, $\chi = 0.80$ this ring is similar to [15]. The bistable behavior of the output port, drop port and inside the ring was shown in Fig. 3a, Fig. 3b and Fig. 3c, respectively. The intensity inside the ring is higher than the one at the drop port, and the intensity at the drop port is a bit

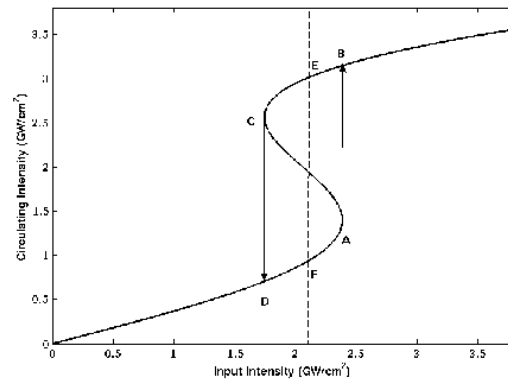
higher the one at the output port. Part of the curves with negative slope represents unstable branch and the arrows show abrupt changes that occur in the outputs at the boundaries of unstable regions A-B (C-D).



(a)



(b)



(c)

Fig. 3 Bistable characteristics of a silicon ring resonator a) at the output channel b) at the drop channel c) inside the ring

The bistable behavior in microring resonators can change by several parameters, by varying the coupling coefficient [15] or by varying the wavelength [11]. The bistable behavior of silicon ring resonators depends on the operating wavelength, Fig.4 shows the effect of the incident wavelength on the

hysteresis behavior inside the ring. It can be noticed that a decrease in λ from 1550 to 1546 nm changes the bistability behavior, such that in $\lambda = 1546$ nm bistability will disappear.

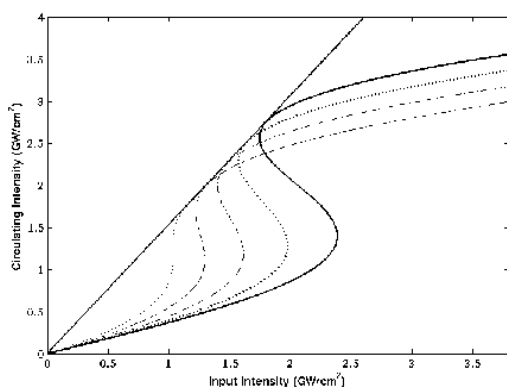


Fig. 4 Bistable behavior inside the silicon ring resonator with $5\mu\text{m}$ radii at $\lambda = 1550$ (solid curve), $\lambda = 1549$ (bold dotted curve), $\lambda = 1548$ (dash-dot curve), $\lambda = 1547$ (dashed curve), $\lambda = 1546$ (pale dotted curve), solid slope line shows field enhancement inside ring for resonance wavelength

It is worth pointing out that in this paper, the bistable behavior of the inside ring was earned by using an analytical theory for optical bistability inside microring resonators [11], while in [9] the bistable behavior of the inside ring was earned by solving a third-order polynomial equation for intensity.

V. DISCUSSION

With reference to Fig. 1, let both MR1 and MR2 be in the off state, hence the input bias (E_{bias}) goes to the output port, E_{bias} is initially red tuned to the both microrings MR1 and MR2. The presence of a CW signal, which is called *set*, at 1550nm with amplitude greater than the input intensity for turning on MR1 (point A in Fig. 3(c)) at the input set port causes to switch MR1 into the on state.

According to Fig. 3(c), after that *set* signal is coupled to MR1 by increasing the input field intensity up to the point A, an increase in the field intensity in the microring is produced (point B). At point A, the instability due to the positive feedback causes a jump to the BE branch [9]. Because of Kerr effect the refractive index will change in such a way which cause to red shift of resonance wavelength of MR1 enough to bring the bias light into the MR1, therefore Q will be on. In the bistable region, when the incident power is decreased, the field intensity in the microring is intense enough to maintain resonance between the microring and input frequency and therefore, hysteresis behavior occurs. Therefore, when *Set* is turned off, MR1 is still in the previous situation with red shifted in wavelength by bias light which is routed into the Q port. When the incident power to the bistable microring decreases and reaches the C point on the BE branch due to the positive feedback, a jump down to the point D occurs, and the ring will be off [9]. MR1 remains on until a *reset* signal turns on the input reset port.

The *reset* causes a change in the refractive index of MR2 red shifting in resonance wavelength enough to bring the bias light into MR2 and turns it on. Therefore, the Bias signal, before arriving to MR1, will couple to MR2 and \bar{Q} will be on. Since MR2 is not in bistability region, after turning off the *reset*, MR2 also turns off and the bias light goes back to the waveguide.

The *set* signal should turn on in t_{MR1} ps before turning off the *reset* ($t_{MR1} = 15$ ps is the time required for turning on MR1 by *set* signal), after turning off *reset*, the bias will couple to MR1 and Q will be on again.

Transfer matrix analysis (TMA) [19], [20] allows to calculate the red shift of resonance wavelength of microrings MR1 and MR2. In Fig. 5, the resonance wavelength and the wavelength red shift of both MR1 and MR2 silicon ring resonator with $5\mu\text{m}$ radii are reported; as shown in the figure, E_{bias} ($\lambda = 1561.94\text{nm}$) can couple to MR1 (or MR2) after turning on the *set* signal (or the *reset* signal).

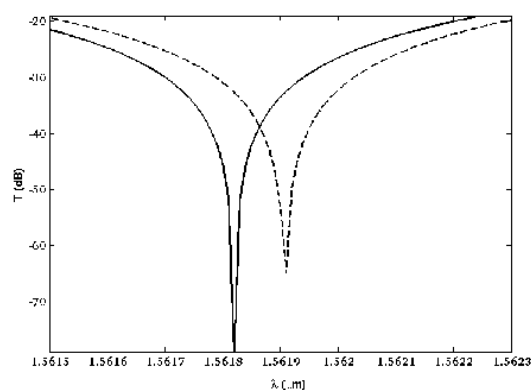


Fig. 5 Resonance wavelength of MR1 (MR2) showing only one of its resonances: $\lambda = 1561.84\text{nm}$ and red shift $\lambda = 1561.94\text{nm}$. The solid line is the resonance wavelength of the ring, the dashed line is the shift wavelength, in MR1 with $23.8\text{GW}/\text{cm}^2$ incident intensity at 1550nm (*set*), in MR2 with $20.5\text{GW}/\text{cm}^2$ incident intensity at 1518nm (*reset*). T(db) is the corresponding output power

VI. CONCLUSION

We have proposed an all-optical set-reset flip-flop by exploiting the bistability behavior of two SOI microrings with the same radius. The bistability behavior of a double coupler microring resonator based on SOI was analyzed, showing that the bistability behaviors are caused by the feedback mechanism and the nonlinear Kerr effects. By changing the CW wavelength, the refractive index of the resonators is temporarily altered through the Kerr effect and the bistability characteristics of the rings takes place. The switching of the bias light into each microring causes to turn on the output signals, thus yielding a flip-flop behavior for device.

ACKNOWLEDGMENT

This work has been partially supported by Regione Liguria P.O. C.R.O. FSE 2007-2013 PhD grant "Nonlinear integrated

photonic devices for optical communication systems”.

REFERENCES

- [1] A. R. Bahrapour, S. Mohammad Ali Mirzaee, F. Farman and S.S. Zakeri, “All-optical flip-flop composed of a single nonlinear passive microring coupled to two straight waveguides,” *Elsevier, Opt. Commun. J.*, vol. 282, pp. 427-433, 2009.
- [2] L. Liu, R. Kumar, K. Huybrechts, T. Spuesens, G. Roelkens, E. J. Geluk, T. Vries, P. Regreny, D. Thourhout, R. Baets and G. Morthier “An ultrasmall, low-power, all-optical flip-flop memory on a silicon chip,” *Nature Photon.*, vol. 4, pp. 182–187, Jan. 2010.
- [3] A.R. Bahrapour, A. Ghadi, R. Farrahi-Moghaddam and F. Sobbatzadeh, “All-optical flip-flop by nonlinear coupling of microring and waveguide,” *Elsevier, Opt. Commun. J.*, vol. 281, pp. 4504-4508, May. 2008.
- [4] T. A. Ibrahim, R. Grover, L. C. Kuo, S. Kanakaraju, L.C. Calhoun and P. T. Ho, “All-Optical Switching in a Laterally Coupled Microring Resonator by Carrier Injection,” *IEEE Photon. Technol. Lett.*, vol. 15, no. 1, pp. 36–38, Jan. 2003.
- [5] M. Takenaka and Y. Nakano, “Realization of All-Optical Flip-Flop Using Directionally Coupled Bistable Laser Diode,” *IEEE Photon. Technol. Lett.*, vol. 16, no. 1, pp. 45–47, Jan. 2004.
- [6] H.J.S. Dorren, D. Lenstra, Y. Liu, M. T. Hill and G. D. Khoe, “Nonlinear Polarization Rotation in Semiconductor Optical Amplifiers: Theory and Application to All-Optical Flip-Flop Memories,” *IEEE J. Quantum Electron.*, vol. 39, no. 1, pp. 141–148, Jan. 2003.
- [7] Y. Liu, M.T. Hill, H. de Waardt, G.D. Khoe, D. Lenstra and H.J.S. Dorren, “All-optical flip-flop memory based on two coupled polarisation switches,” *Electron. Lett.* vol. 38, no. 16, pp. 904–906, Aug. 2002.
- [8] T. Fukushima and T. Sakamoto, “Kerr-effect-induced S–R flip-flop operation in an optical fiber loop resonator with double couplers,” *Opt. Lett.* vol. 20, no. 10, pp. 1119–1121, May. 1995.
- [9] A.R. Bahrapour, M. Karimi, M.J. Abolfazli Qamsari, H. Rooholamini Nejad and S. Keyvaninia, “All-optical set–reset flip–flop based on the passive microring-resonator bistability,” *Elsevier, opt. commun. J.*, vol. 281, pp. 5104-5113, Jul. 2008.
- [10] A. Trita, S. Furst, G. Mezosi, M. Sorel, M. Vidal, J. Yu, F. Bragheri, I. Cristiani and G. Giuliani, “Time-domain response to ps optical pulse trigger of an all-optical flip-flop based on semiconductor ring laser,” *SPIE*, vol. 6997, pp. 699724-1 -699724-6, 2008.
- [11] I. D. Rukhlenko, M. Premaratne, and G. P. Agrawal, “Analytical study of optical bistability in silicon ring resonators,” *Opt. Lett.* vol. 35, no. 1, pp. 55–57, Jan. 2010.
- [12] X. Zheng, Y. Luo, G. Li, I. Shubin, H. Thacker, J. Yao, K. Raj, J. E. Cunningham, and A. V. Krishnamoorthy, “Enhanced optical bistability from self-heating due to free carrier absorption in substrate removed silicon ring modulators,” *OSA. OpEx.* vol. 20, no. 10, pp. 11478- 11486, May. 2012.
- [13] K. Ikeda R. E. Saperstein, N. Alic, and Y. Fainman, “Thermal and Kerr nonlinear properties of plasma-deposited silicon nitride/silicon dioxide waveguides,” *OSA. OpEx.* vol. 16, no. 17, pp. 12987–12994, Aug. 2008.
- [14] B. A. Daniel and G. P. Agrawal, “Phase-Switched All-Optical Flip-Flops Using Two-Input Bistable Resonators,” *IEEE. Lett.PTL* .vol.24, no.6, pp.479-481, Mar. 2012.
- [15] B. Vanishkorn, C. Kusalajeerung, S. Chiangga, S. Pitukwongsaporn, B. Jukgoljun, and P. P. Yupapin, “Linear And Nonlinear Behaviors Of Light In A Silicon Ring Resonator,” *Wiley. Motl.* vol. 53, no. 5, pp. 997-1000, May. 2011.
- [16] Q. Lin, O. J. Painter, and G. P. Agrawal, “Nonlinear optical phenomena in silicon waveguides: Modeling and applications,” *OSA. OpEx.* vol. 15, no. 25, pp. 16604-16644, Nov. 2007.
- [17] V.R. Almeida, and M. Lipson, “Optical bistability on a silicon chip,” *Opt. Lett.* vol. 29, no. 20, pp. 2387-2389, Oct. 2004.
- [18] Q. Xu, and M. Lipson, “Carrier-induced optical bistability in silicon ring resonator,” *Opt. Lett.* vol. 31, no. 3, pp. 341-343, Feb 2006.
- [19] J. K. S.Poon, J. Scheuer, S. Mookherjea, G. T.Paloczi, Y. Huang, and A. Yariv, “Matrix analysis of microring coupled -resonator optical waveguides,” *OSA. OpEx.* vol. 12, no. 1, pp. 90-103, Jan. 2004.
- [20] W. Shang, C. Berkehan and W. Hui, “Microring-based optical pulse-train generator,” *OSA. OpEx.* vol. 18, no. 18, pp. 19314-19323, Sep. 2010.